Sulfonated activated carbons as potential catalysts for biolubricant synthesis

Aurélia R. O. Ferreira[a], Joaquín Silvestre-Albero[b], Martin E. Maier[c], Nágila M. P. S. Ricardo[d], Célio L. Cavalcante Jr[a] and F. Murilo T. Luna[a†]

[a]Núcleo de Pesquisas em Lubrificantes,Grupo de Pesquisa em Separações por Adsorção,Depto. de Engenharia Química, Universidade Federal do Ceará, Campus do Pici, Bl. 709, Fortaleza, CE, 60440-900, Brazil.

[b]Laboratorio de Materiales Avanzados, Depto. de Química Inorgánica, Universidad de Alicante, E-03690 San Vicente del Raspeig, Spain.

[c]Fachbereich Chemie, Institut für Organische Chemie, Auf der Morgenstelle 18,Tübingen, 72076, Germany.

[d]Laboratório de Polímeros e Inovação de Materiais, Depto.de Química Orgânica e Inorgânica, Universidade Federal do Ceará, Campus do Pici, Bl. 940, Fortaleza, CE, CEP 60440-900, Brazil.

[†] Corresponding author (Phone: +55-85-3366-9611, Fax: +55-85-3366-9601, e-mail: murilo@gpsa.ufc.br)

ABSTRACT

In this study, sulfonated activated carbons have been prepared, under different conditions, with the purpose of evaluating the effect of the nature and amount of sulfonic surface groups on the esterification reaction of free fatty acids (FFA) with different long-chain alcohols. The synthesized catalysts were characterized using different techniques and ^{1}H NMR was used for monitoring the reaction products. The modifications of the surface functionalities were assessed by X-ray Photoelectron Spectroscopy (XPS) and Thermogravimetric analysis (TGA), while changes in the porous network and morphology of the samples were evaluated before and after the treatment of the original activated carbon sample. XPS results showed the presence of two types of sulfur, one from thiophenic sulfur (present on all materials, including the unmodified sample), and the other from sulfonic groups (SO_3H), at 168 eV (present only in the modified samples). These catalysts were applied in the esterification reaction and presented excellent catalytic performances, while the original activated carbon exhibited conversions similar to reactions without any catalyst. On the other hand, the conversion of fatty acids when using the modified carbons improves significantly with values up to ~100 % to mono alcohols and 70 % to trimethylolpropane.

Keywords: activated carbon; sulfonation; esterification; oleic acid; biolubricants.

1. INTRODUCTION

Lubricants constitute an enormous market worldwide, their consumption being mainly in the automotive industry [1]. An interesting approach that would help in reducing the impact caused by petroleum derivatives and their anthropogenic impact to the environment is the use of lubricants obtained from vegetable oils. Since the 1980s, the trend in bio-based lubricants has been to overcome the limitations of the oils derived from plants, e.g. by chemical modification of these oils, or the synthesis of esters that may be partially derived from renewable resources [2]. The vegetable oils are formed by fatty acids that may be used to synthesize new bio-based lubricants. In general, the fatty acids comprise about 85 % of the vegetable oils, thus making them the major factor for their physicochemical properties. Their chain lengths and the number of double bonds are important features for the melting point, stability and viscosity of the final products [3].

Nevertheless, a lot of research has been done on the exploration of new feedstocks and modification methods, development of more efficient catalysts for chemical modification of fatty acids, for example oleic acid, and optimization of the modification approaches, using diols, polyols as well as linear and branched alcohols [4-6]. Chemical modifications are mainly devoted to reactions on the carboxylic functional group and double bonds present in the oil. One way is to obtain new esters from triglycerides through transesterification or hydrolysis/esterification to obtain new products with improved physicochemical properties for lubrication applications [7]. The reaction between carboxylic acid and alcohol is used for the synthesis of drugs, solvents, perfumes and biofuels [8]. Normally, this reaction is carried out with short chain alcohols such as methanol and ethanol [9-11]. However, long chain alcohols (between C8 and C14) with linear or branched carbon chain or a polyol are considered more interesting for the production of esters that are used as basestocks oil for lubricants formulation. These types of long chain alcohols, when used to produce bio-based lubricants, have a large influence on the properties of the final products, such as viscosity, pour point, oxidative stability and others [12].

Catalytic esterification of free fatty acids or carboxylic acid usually works over Brønsted acids such as H_2SO_4, HCl, HF, among others. A problem with these catalysts is the difficulty to remove them from the reaction mixture after their use. In addition, the liquid acid can be corrosive to the reactor and produce large amounts of acidic waste water. To try to overcome the problem inflicted by the homogenous catalysts, several studies have used carbonaceous materials with potential application in catalysis. These materials are frequently chemically modified with the purpose to obtain improved catalytic activity, selectivity and stability when dealing with reactions to obtain bioproducts [8, 13-20].

In this study, activated carbons were modified to be used as catalyst in the esterification reaction of free fatty acids (FFA) with different long-chain alcohols (octanol, 2-ethylhexanol and trimethylolpropane). The kinetics of each reaction and selectivity measurements were carried out for all catalysts. The original and the sulfonated activated carbons were characterized by X-ray Photoelectron Spectroscopy (XPS), Fourier Transformed Infrared Spectroscopy (FTIR), N_2 adsorption/desorption, Thermogravimetric analysis (TGA) and Scanning Electron Microscopy (SEM) to evaluate the changes in the surface, the morphology and the porous structure of the catalysts.

2. EXPERIMENTAL SECTION

2.1. Materials

Activated carbon (GAC 1240 PLUS) was provided by Norit (Netherlands). Octanol (>99 wt.%), trimethylolpropane (>98 wt.%), 2-ethyhexanol (>99.6 wt.%) and deuterated chloroform ($CDCl_3$, 99.8 %) were purchased from Sigma-Aldrich (USA). Oleic acid (C18:1, >98 wt.%) was provided by VETEC (Brazil) and used as FFA model for the esterification reactions. Analytical grade reagents (hydrochloric acid and sulfuric acid) were purchased from Dinâmica (Brazil).

2.2. Modification and characterization of the activated carbon

The sulfonic groups were introduced by aromatic electrophilic substitution (Figure 1). In a first step, the activated carbon (AC) sample was washed with hydrochloric acid (0.1 mol/L) in deionized water until neutral pH, and then oven-dried at 110 °C for 24 h. The AC sample was subsequently chemically treated with sulfuric acid. The treatment was carried out using 5 g of AC with 50 mL of concentrated sulfuric acid, under reflux at 100 ºC, 150 ºC and 200 ºC (labeled ACS1, ACS2 and ACS3, respectively) for 5 h. All materials were then repeatedly washed with deionized water until neutral pH and dried at 110 °C for 24 h.

<Figure 1>

Textural properties were evaluated by nitrogen adsorption at -196 ºC in Autosorb IQ3 from Quantachrome Instruments (USA). Approximately 40 mg of sample were degassed under vacuum with the aid of a turbo-molecular pump, heated from room temperature to 150 °C for 6 h, heating rate: 1 °C/min. The specific surface area (S_{BET}) was calculated using the BET method and micropore volume was determined using the Dubinin–Radushkevich (DR) equation. The mesopore volume was obtained by subtracting the micropore volume from the total pore volume. The pore size distributions were calculated using the density functional theory method (DFT), following the approach reported by Jaciello and Thommes [21].

The infrared spectra were recorded on an ABB Bomem FTLA 2000-102 FTIR instrument (USA). The spectra were acquired by accumulating 100 scans at 4 cm^{-1} resolution in the range of 400-4000 cm^{-1}using samples (2 wt.%) with KBr.

The study of the morphology was carried out by scanning electron microscopy using Inspect S50 (FEI, USA) in the magnification range between 500 and 10000. The preparation of the samples was carried out by dispersing it on a carbon tape, and then metalizing it with Au. Energy Dispersive

X-Ray Spectroscopy (EDS), measured with the SEM, was used to evaluate the elemental content of the original and modified samples.

Thermal stability of catalysts was measured by thermal gravimetric analysis (TGA-QMS customized, model STA 409 CD/403/5/G SKIMMER – Netzsch, Germany) with a heating ramp of 10 °C/min, from 30 °C to 800 °C.

X-ray photoelectron spectra (XPS) were collected using a K-Alpha spectrometer from Thermo Scientific (USA). All spectra were collected using Al-Kα radiation (1486.6 eV), monochromatized by a twin crystal monochromator, yielding a focused X-ray spot (elliptical in shape with a major axis length of 400 μm) at 3 mA × 12 kV. The alpha hemispherical analyzer was operated in the constant energy mode with survey scan pass energies of 200 eV to measure the whole energy band and 50 eV in a narrow scan to selectively measure the particular elements. Charge compensation was achieved with the system flood gun that provides low energy electrons and low energy argon ions from a single source. The C 1s core level was used as reference binding energy, and it is located at 284.6 eV. The powder samples were pressed and mounted on the sample holder and placed in the vacuum chamber. Before recording the spectrum, the samples were maintained in the analysis chamber until a residual pressure of *ca.* 5×10^{-7} N/m^2 was reached. The quantitative analysis was estimated by calculating the integral of each peak, after subtracting the S-shaped background, and by fitting the experimental curve to a combination of Lorentzian (30 %) and Gaussian (70 %) lines.

2.3. Catalytic experiments

The catalytic activities in the esterification reaction of oleic acid (OA) with octanol (OcA), 2-ethylhexanol (EhA) and trimethylolpropane (TMP) were carried out under inert atmospheric at 90 °C using a catalyst/oleic acid ratio of 4.0 wt.% and stirring of 500 rpm. The molar ratios of monoalcohols (OcA and EhA) to oleic acid were 4:1. For the TMP, the molar ratio was 1:4

(TMP:OA). The reaction experiments were carried out until 6 h. The products of the esterification reaction were evaluated by Nuclear Magnetic Resonance of Hydrogen (^{1}H NMR) obtained on Bruker model AVANCE spectrometers operating at a frequency of 400 MHz. The solvent used for the NMR measurements was deuterated chloroform at a temperature of 25 °C. The equations and calculations are described below as well as the reference peaks for each calculation.

The peak of the -CH_2- bond, at approximately 2.25-2.5 ppm, was taken as reference in the conversion calculations and the peak for the -HC=CH- bond was used for the selectivity calculations using Eqs. 1-3:

$$CO = \frac{a_1}{2}.100\% \quad (1)$$

$$DC = \frac{2-a_2}{2}.100\% \quad (2)$$

$$S = \frac{CO}{CO+DC}.100\% \quad (3)$$

where: a_1 is the area of the new binding peak, concerning –CH_2– bond, approximately 4.0 ppm; a_2 is the peak area of double bond, approx. 5.5-5.25 ppm; CO is the conversion of oleic acid; DC is the double bond conversion and S is selectivity for oleic ester.

3. RESULTS AND DISCUSSION

3.1. Characterization of modified activated carbons

The N_2 adsorption/desorption isotherms at -196 °C of the catalysts are shown in Figure 2a (data included in Table 1). All materials exhibited a type IV isotherm, according to the IUPAC classification [22], with narrow H4 type hysteresis. This means that the materials are micro-mesoporous carbons, as shown in Figure 2b. Therefore the treatment with sulfuric acid does not affect significantly their total pore volume, however, a decrease in specific surface area was observed for the ACS1 sample, as previously reported [8, 13, 14, 23 and 24]. It can be observed that ACS1 has larger meso-macropore volume than other catalysts. The PSD curves presented in Figure 2b indicated that the modified activated carbons were very similar in terms of pore size distributions.

<Figure 2>

<Table 1>

The type of bond on the surface of the catalysts was evaluated using FTIR (Figure 3), to verify the presence of the sulfonic groups on the surface of the materials through their bonds. The wavenumber between 3500 and 3250 cm^{-1} refers to –OH group, and the region between 1630 – 1730 cm^{-1} is attributed to stretching of –C=C– and –COOH bonds. Sulfonic acid, when in its anhydrous form, absorbs in the second region: 1150-1300 cm^{-1}. However, a displacement is observed in Figure 3 that may be due to the rapid hydration of the sulfonic groups forming hydronium sulfonates in the experimental conditions used in this study [25]. The vibrational band between 1250 and 1000 cm^{-1} refers to the S=O bond [23]. The presence of the C=S bond was confirmed at the wavenumber 1120 cm^{-1} [26] and the stretch remaining at approximately 600 cm^{-1} is due to C-S binding. Therefore, the presence of the sulfonic groups in all modified samples was evidenced.

<Figure 3>

XPS studies were carried out to better evaluate the sulfonic groups in all catalysts (see Figure 4). The high resolution C 1s can be divided into three small peaks at 284.5 eV (C–C/C=C), 285.6 eV (C–O/C–S), and 287.0 eV (O=C), which are present in all samples (Fig. 4a,c,e,g) [8, 26, 27]. The narrow S 2p presents two relative sulfur types of –C–S–C– attributed to thiophenic sulfur (between 163 and 166 eV) [26]. The sulfonic groups SO_3H (168 eV) [26, 28] were observed only in modified samples. Between all catalysts (ACS1, ACS2 and ACS3), the ACS1 stands out for the amount of sulfonic groups on the surface, much higher than the other catalysts (see Table 1).

<Figure 4>

The SEM images of activated carbons modified at different temperatures are shown in Figure 5. The carbons have a completely irregular morphology, in other words, they are amorphous and have a large particle size with a small difference in the sample treated at 150 °C (ACS2) which apparently has more available surface. The EDS results, measured with the SEM, are shown in Table 2. The FTIR results had shown the presence of sulfonic groups already in the original carbon, as shown in Table 2; however, it is observed that the mass percentage of sulfur found in the original AC is lower than in those samples treated with sulfuric acid. There was also an increase in the presence of oxygen which may also be associated with the presence of the $-SO_3H$ groups.

<Figure 5>

<Table 2>

The weight loss curves and those derived from each catalyst sample are presented in Figure 6. All samples exhibit a mass loss up to 100 °C, associated to the loss of water. Also, all catalysts present a mass loss in the region of 300 °C, except the original AC (Figure 6a). Malins *et al.* [6] have associated this loss to the decomposition of SO_3H groups. These results are in compliance with what had been observed for the XPS studies (Table 1).

<Figure 6>

3.2. Catalytic experiments

The catalytic performance was measured by ^1H NMR (Figure 7) trying to identify mainly the products of the esterification reactions. The peak at approximately 5.25-5.5 ppm is related to the

protons of the double bond (-HC=CH-) of the oleic acid molecule and the peak at 2.25-2.5 ppm refers to the hydrogen of the -CH_2- group near the carbonyl group. The esterification reaction is confirmed in Figure 7 with the appearance of the peak at 4.0 ppm. As the alcohol had an excess, for reactions with octanol and 2-ethyhexanol, the peak about 3.5 ppm is referring to –CH– related to oxygen, as shown in Figure 7a,b.

<Figure 7>

The results of the conversion over time, for esterification reaction using octanol, 2-ethylhexanol and TMP, are presented in Figure 8, 9 and 10, respectively. For all experiments, the AC sample exhibit a low catalytic activity in the oleic acid esterification, with conversion values close to results of the non-catalytic process, meaning there was no specific catalytic action. The catalytic results reveal that all sulfonated samples showed excellent conversion values. For octanol, all samples presented similar results (conversion ≈ 100 % after *ca.* 100 min). However, for 2-ethylhexanol (Figure 9) and TMP (Figure 10), the ACS1 sample (most sulfonated one) displayed higher conversion values than the others (ACS2 and ACS3).

Although the ACS1 stands out among the catalysts, it exhibits oleic acid conversion value of ~70 % when using TMP (Figure 10). This may be due to a decrease of the nucleophilicity of the alcohol, a steric effect and lower vapor pressure, all these effects would lead to lower conversion values [12, 29-31].

<Figure 8>

<Figure 9>

<Figure 10>

The selectivities to esters are presented in Figure 11. Despite the branching of 2-ethylhexanol, the catalysts were more selective in this reaction reaching 90 % when ACS2 was used. However, the selectivity to esters was 48 % when TMP alcohol was used on ACS2 catalyst. The values of selectivities to esters showed decreasing trend with increasing branching level of alcohols (octanol<2-ethylhexanol<TMP), for non-modified catalyst (AC). The sulfonated catalysts showed better performances than AC for all alcohols. Thus, the selectivity to esters increased with the presence of the sulfonated catalyst, in all cases in such a way that the modified catalysts exhibited similar selectivity trend (2-Ethylhexyl oleate>Octyl oleate>TMP oleate) after 6 h of reaction. On the one hand, increasing the sulfonic groups and meso-macropore volume in the catalysts (ACS1>ACS2>ACS3), as checked by textural properties and XPS results, the selectivity to obtain TMP trioleate was improved with respect to original AC.

<Figure 11>

4. CONCLUSIONS

Sulfonated activated carbons were prepared by aromatic electrophilic substitution. The results of N_2 physisorption and MEV showed that the treatment with sulfuric acid did not change significantly the structure of the materials. However, changes in micropore volume of sulfonated activated carbons were observed. The presence of sulfonic groups was evidenced by XPS and TGA, in the peak S 2p at 168 eV and an additional region of weight loss at 300 ºC, respectively. The XPS results exhibited the occurrence of two types of sulfur, one from thiophenic sulfur (present on all materials, including the unmodified sample), and the other from sulfonic groups (SO_3H), at 168 eV (present only in the modified samples).

The catalytic results in the esterification reaction of oleic acid with three different alcohols were very promising. The original AC showed no significant effect when compared with a non-catalytic process. Nevertheless, the difference is quite discrepant when using the modified carbons (ACS1, ACS2 and ACS3). Conversions values for these catalysts reached approximately 100 % when the mono alcohols were used, with excellent selectivity (up to 90 %). However, the ACS1 sample revealed better performance in obtaining the ester of TMP with selectivity above of 60 %, due mainly the high content of sulfonic groups and meso-macropore volume in this catalyst.

ACKNOWLEDGMENT

The authors wish to acknowledge the financial support provided by CNPq (*Conselho Nacional de Desenvolvimento Científico e Tecnológico*). This study was financed in part by the *Coordenação de Aperfeiçoamento de Pessoal de Nível Superior* (CAPES) – Brazil – Finance Code 001. FMTL and JSA acknowledge financial support from the University of Alicante (INV19-18). Also, financial support from MINECO (MAT2016-80285-p), GV (PROMETEOII/2014/004), and H2020 (MSCA-RISE-2016/NanoMed Project) is gratefully acknowledged.

REFERENCES

[1] T. Mang, W. Dresel, Lubricants and Lubrication, 2end Ed, Wiley-VCH, Weinheim, 2007.

[2] M.P. Schneider, Plant-oil-based lubricants and hydraulicfluids, J. Sci. Food Agric. 86 (2006) 1769-1780. https://doi.org/10.1002/jsfa.2559.

[3] R. Garcés, E. Martínez-Force, J.J. Salas, Vegetable oilbasestocksforlubricants, Grasas y Aceites. 62 (2011) 21-28. https://doi.org/10.3989/gya.045210.

[4] H. Wagner, R. Luter, T. Mang, Lubricant base fluids based on renewable raw materials. Their catalytic manufacture and modification, Appl. Catal. A Gen. 221 (2001) 429–442. https://doi.org/10.1016/S0926-860X(01)00891-2.

[5] H.A. Hamid, R. Yunus, U. Rashid, Synthesis of palm oil-based trimethylolpropane ester as potential biolubricants: Chemical kinetics modeling, Chem. Eng. Journal 200–202 (2012) 532–540. https://doi.org/10.1016/j.cej.2012.06.087.

[6] J. Salimon, N. Salih, E. Yousif, Biolubricant basestock from chemical modified ricinoleic acid, J. King Saud Univ. Sci. 24, (2012) 11–17. https://doi.org/10.1016/j.jksus.2010.08.008.

[7] J. McNutt, Q. (Sophia) He, Development of biolubricants from vegetable oils via chemical modification, J. Ind. and Eng. Chem. 36 (2016) 1–12. https://doi.org/10.1016/j.jiec.2016.02.008.

[8] A. Aldana-Pérez, L. Lartundo-Rojas, R. Gómez, M.E. Niño-Gómez, Sulfonic groups anchored on mesoporous carbon Starbons-300 and its use for the esterification of oleic acid, Fuel 100 (2012) 128–138. https://doi.org/10.1016/j.fuel.2012.02.025.

[9] M. Hümmer, S. Kara, A. Liese, I. Huth, J. Schrader, D. Holtmann, Synthesis of menthol fatty acid esters in and from menthol and fatty acids novel concept for lipase catalyzed esterification based on eutectic solvents, Molecular Catalysis 458 (2018) 67–72. https://doi.org/10.1016/j.mcat.2018.08.003.

[10] A.L. de Lima, J.S.C. Vieira, C.M. Ronconi, C.J.A. Mota, Tailored hybrid materials for biodiesel production: Tunning the basetype, support and preparation method for the best catalytic performance, Molecular Catalysis 458 (2018) 240-246. https://doi.org/10.1016/j.mcat.2017.09.032.

[11] M. Jin, M. Choi, Hydrothermal deoxygenation of triglycerides over carbon supported bimetallic PtRe catalysts without an external hydrogen source, Molecular Catalysis 474 (2019) 110419. https://doi.org/10.1016/j.mcat.2019.110419.

[12] R.M.A. Saboya, J.A. Cecilia, C. García-Sancho, F.M.T. de Luna, E. Rodríguez-Castellón, C.L. CavalcanteJr, WO3-based catalysts supported on porous clay heterostructures (PCH) with Si–Zr pillars for synthetic esters production, Applied Clay Science 124–125 (2016) 69-78. https://doi.org/10.1016/j.clay.2016.02.004.

[13] S. Niu, Y. Ning, C. Lu, K. Han, H. Yu, Y. Zhou, Esterification of oleic acid to produce biodiesel catalyzed by sulfonated activated carbon from bamboo, Energy Conversion and Management 163 (2018) 59–65. https://doi.org/10.1016/j.enconman.2018.02.055.

[14] K. Malins, V. Kampars, J. Brinks, I. Neibolte, R. Murnieks, Synthesis of activated carbon based heterogenous acid catalyst for biodiesel preparation, Applied Catalysis B: Environmental 176–177 (2015) 553–558. http://dx.doi.org/10.1016/j.apcatb.2015.04.043.

[15] Z. Gao, S. Tang, X. Cui, S. Tian, M. Zhang, Efficient mesoporous carbon-based solid catalyst for the esterification of oleic acid, Fuel 140 (2015) 669–676. https://doi.org/10.1016/j.fuel.2014.10.012.

[16] J.M.R. Gallo, R. Alamillo, J.A. Dumesic, Acid-functionalized mesoporous carbons for the continuous production of 5-hydroxymethylfurfural, Journal of Molecular Catalysis A: Chemical 422 (2016) 13–17. http://dx.doi.org/10.1016/j.molcata.2016.01.005.

[17] D. Mun, A.T. Hoang Vo, B. Kim, Yong-Gun Shul, J.K. Cho, Solventless esterification of fatty acids with trimethylolpropane using sulfonated amorphous carbons derived from wood powder, Catalysis Communications 96 (2017) 32–36. https://doi.org/10.1016/j.catcom.2017.03.015.

[18] M. Gonçalves, M. Mantovani, W.A. Carvalho, R. Rodrigues, D. Mandelli, J.S. Albero, Biodiesel wastes: An abundant and promising source for the preparation of acidic catalysts for utilization in etherification reaction, Chemical Engineering Journal 256 (2014) 468–474. https://doi.org/10.1016/j.cej.2014.07.013.

[19] Zhichao Miao, Zhenbin Li, Jinping Zhao, Weijiang Si, Jin Zhou, Shuping Zhuo, MoO_3 supported on ordered mesoporous zirconium oxophosphate: An efficient and reusability solid acid catalyst for alkylation and esterification, Molecular Catalysis 444 (2018) 10-21. http://dx.doi.org/10.1016/j.mcat.2017.10.028.

[20] S. He, W. Wang, Z. Shen, G. Li, J. Kang, Z. Liu, Gui-Chang Wang, Q. Zhang, Y. Wang, Carbon nanotube-supported bimetallic Cu-Fe catalysts for syngas conversion to higher alcohols, Molecular Catalysis 479 (2019) 110610. https://doi.org/10.1016/j.mcat.2019.110610.

[21] J. Jaciello, M. Thommes, Comparison of DFT characterization methods based on N2, Ar, CO2, and H2 adsorption applied to carbons with various pore size distributions, Carbon 42 (2004) 1227-1232. https://doi.org/10.1016/j.carbon.2004.01.022.

[22] M. Thommes, K. Kaneko, A.V. Neimark, J.P. Olivier, F. Rodriguez-Reinoso, J. Rouquerol, K.S.W. Sing, Physisorption of gases, with special reference to the evaluation of surface area and pore size distribution (IUPAC Technical Report), Pure Appl. Chem. 87(9-10): (2015) 1051–1069. https://doi.org/10.1515/pac-2014-1117.

[23] T.K. Mahto, R. Jain, S. Chandra, D. Roy, V. Mahto, S.K. Sahu, Single step synthesis of sulfonic group bearing graphene oxide: A promising carbo-nano material for biodiesel production, Jour. of Env. Chem. Eng., v. 4, (2016) 2933-2940. http://dx.doi.org/10.1016/j.jece.2016.06.006.

[24] P. Maneechakr, J. Samerjit, S. Karnjanakom, Ultrasonic-assisted biodiesel production fromwaste cooking oil over novel sulfonic functionalized carbon spheres derived from cyclodextrin via one-step: a way to produce biodiesel at short reaction time, RSC Adv., 5 (2015) 55252. http://dx.doi.org/10.1039/C5RA09499B.

[25] S.M. de Rezende, B.G. Soares, F.M.B. Coutinho, S.C.M. dos Reis, M.G. Reid, E.R. Lachter, R.S.V. Nascimento, Aplicação de Resinas Sulfônicas como Catalisadores em Reações de Transesterificação de Óleos Vegetais, Polimeros: Ciência e Tecnologia vol.15, n3, (2005) 186-192. http://dx.doi.org/10.1590/S0104-14282005000300008.

[26] Y. Yao, Y. Guo, W. Du, X. Tong, X. Zhang, In situ synthesis of sulfur-doped graphene quantum dots decorated carbon nanoparticles hybrid as metal-free electrocatalyst for oxygen reduction reaction, Journal of Materials Science: Materials in Electronics. 29, (2018) 17695–17705. https://doi.org/10.1007/s10854-018-9875-5.

[27] T.V. Tam, S.G. Kang, K.F. Babu, Eun-Suok Oh, S.G. Lee, W.M. Choi, Synthesis of B-doped graphene quantum dots as a metal-free electrocatalyst for the oxygen reduction reaction, Journal of Materials Chemistry A, 5 (2017) 10537–10543. https://doi.org/10.1039/C7TA01485F.

[28] R.M.A. Saboya, J.A. Cecilia, C. García-Sancho, A.V. Sales, F.M.T. de Luna, E. Rodríguez-Castellón, C.L. Cavalcante Jr, Assessment of commercial resins in the biolubricants production from free fatty acids of castor oil, Catalysis Today 279 (2017) 274–285. http://dx.doi.org/10.1016/j.cattod.2016.02.020.

[29] F.M. Fadzel, J. Salimon, D. Derawi, Synthesis Of TMP-Ester Biolubricant Basestock From Palm Stearin Fatty Acids, AIP Conference Proceedings 1940, 020095 (2018). https://doi.org/10.1063/1.5028000.

[30] N. Mohd Nor, D. Derawi, J. Salimon, Synthesis of Palm Oil Fatty Acid and Trimethylolpropane Based Ester for Biolubricant Base Stocks, AIP Conference Proceedings 1940, (2018) 020085. https://doi.org/10.1063/1.5028010.

[31] Kalliopi V. Avramidou, Federica Zaccheria, Stamatia A. Karakoulia, Kostas S. Triantafyllidis, NicolettaRavasio, Esterification of free fatty acids using acidic metal oxides and supported polyoxometalate (POM) catalysts, Molecular Catalysis 439 (2017) 60–71. https://doi.org/10.1016/j.mcat.2017.06.009.

376 **TABLE CAPTIONS**

377

378 **Table 1.** Textural properties of samples (AC, ACS1, ACS2 and ACS3).

379 **Table 2.** Elemental content of the original and modified samples from the EDS measurements.

380

Table 1

	AC	**ACS1**	**ACS2**	**ACS3**
S_{BET} (m^2/g)	931	714	954	869
Total pore volume (cm^3/g)	0.454	0.468	0.483	0.440
Micropore volume, DR* (cm^3/g)	0.397	0.335	0.419	0.400
Meso-macropore volume (cm^3/g)	0.057	0.133	0.064	0.040
Atomic percentage of S (%) From SO_3H (at 168 eV)**	-	0.36	0.17	0.20

* Dubinin-Radushkevich (DR); **Data from XPS.

385 **Table 2**

386

Elements	AC (wt.%)	ACS1 (wt.%)	ACS2 (wt.%)	ACS3 (wt.%)
C	83.8	75.3	80.2	84.6
O	6.2	8.4	7.8	8.4
S	0.7	1.1	1.6	1.6
Si	1.3	1.5	1.0	0.6
Al	1.1	1.1	0.9	0.5
Cl	0.7	0.4	0.5	0.2
K	0.1	0.1	0.1	-

387

388

389

390

391

392

393

394

FIGURE CAPTIONS

Figure 1. Sulfonation of activated carbon (modified from [8]).

Figure 2. (a) Nitrogen adsorption/desorption isotherms at -196 ℃ for all samples; (b) Pore size distribution obtained by DFT.

Figure 3. FTIR spectra of samples AC, AS1, ACS2 and ACS3.

Figure 4. XPS spectra of high-resolution C 1s and S 2p of all catalysts.

Figure 5. Images obtained by scanning electron microscopy of samples (a) AC, (b) ACS1, (c) ACS2 and (d) ACS3.

Figure 6. Mass loss curves and their derivatives:(a) AC, (b) ACS1, (c) ACS2 and(d) ACS3.

Figure 7. ^{1}H NMR of samples obtained after esterification reactions of oleic acid with octanol (a), 2-ethylhexanol (b) and TMP (c) alcohols at 90 ℃. Conditions: 4:1 molar ratio to octanol or 2-ethylhexanol/oleic acid; 1:4 to TMP/oleic acid; 4 wt.% of the catalyst/oleic acid.

Figure 8. Conversion over time of the oleic acid with octanol at 90 ℃. Conditions: 4:1 molar ratio to octanol/oleic acid; 4 wt.% of the catalyst/oleic acid.

Figure 9. Conversion over time of the oleic acid with 2-ethylhexanol at 90 ℃. Conditions: 4:1 molar ratio to 2-ethylhexanol/oleic acid; 4 wt.% of the catalyst/oleic acid.

Figure 10. Conversion over time of the oleic acid with TMP at 90 ℃. Conditions: 1:4 to TMP/oleic acid; 4 wt.% of the catalyst/oleic acid.

Figure 11. Selectivity in oleate esters for experiments of oleic acid with octanol, 2-ethylhexanol and TMP at 90 ℃ (time = 6 h), for all catalysts.

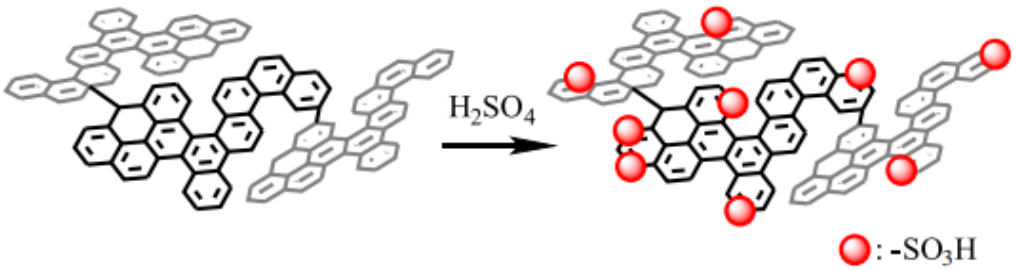

417

418 **Figure 1**

419

(a)

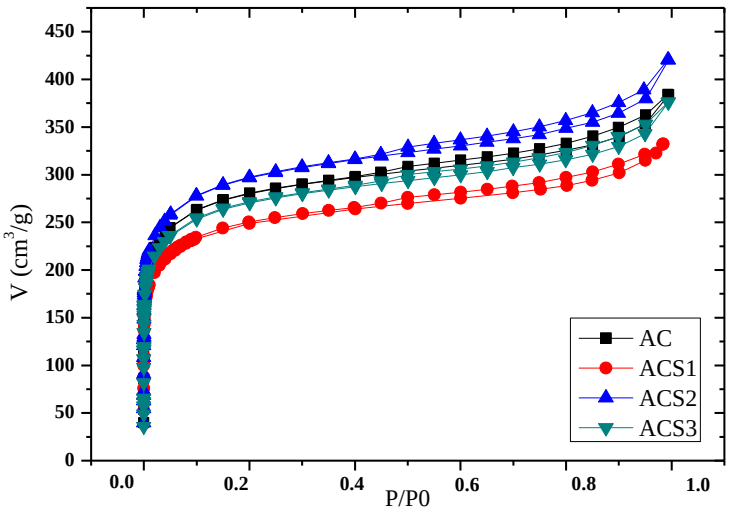

(b)

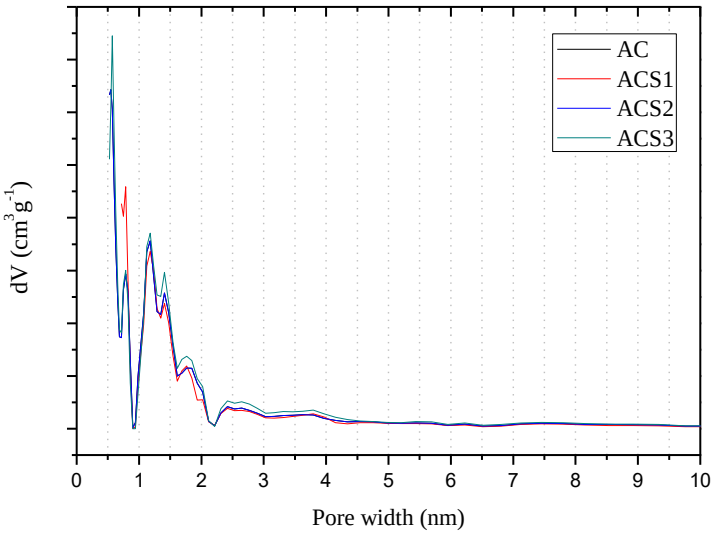

420 **Figure 2**

421

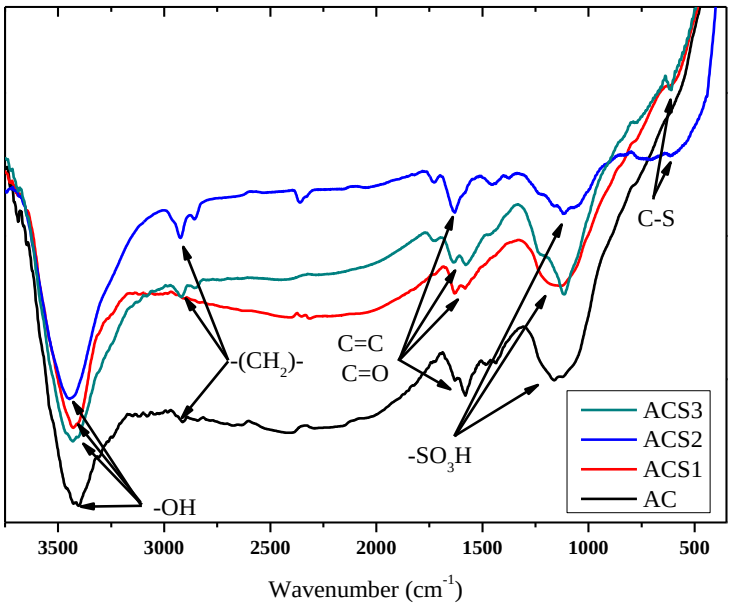

422

423 **Figure 3**

424

(a) AC (C 1s)

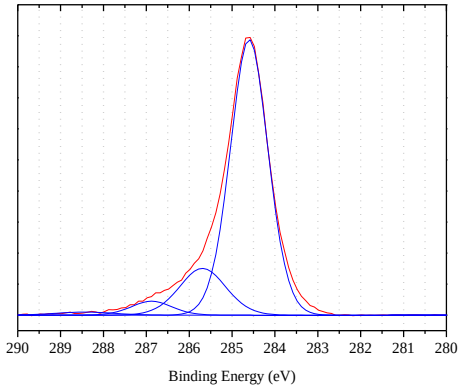

(b) AC (S 2p)

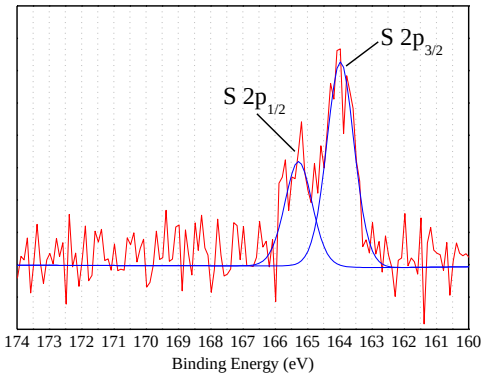

(c) ACS1 (C 1s)

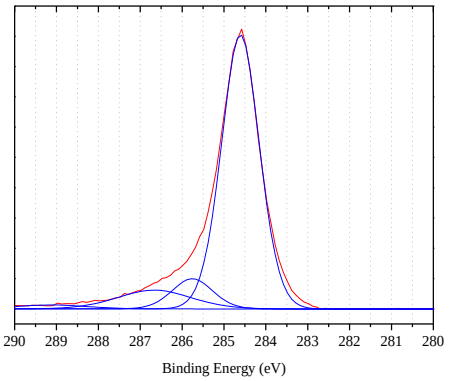

(d) ACS1 (S 2p)

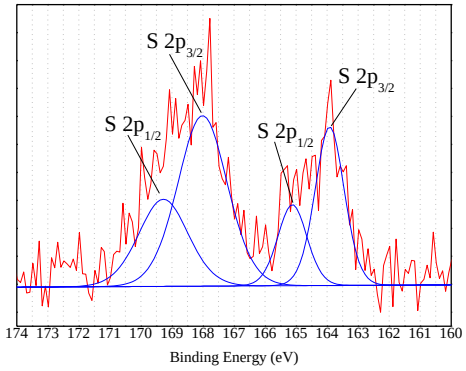

(e) ACS2 (C 1s)

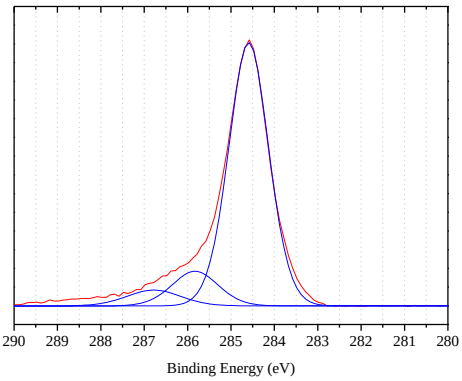

(f) ACS2 (S 2p)

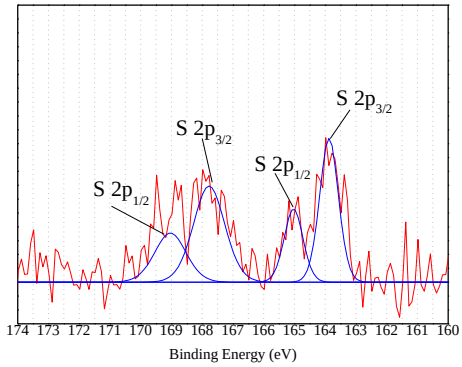

(g) ACS3 (C 1s)

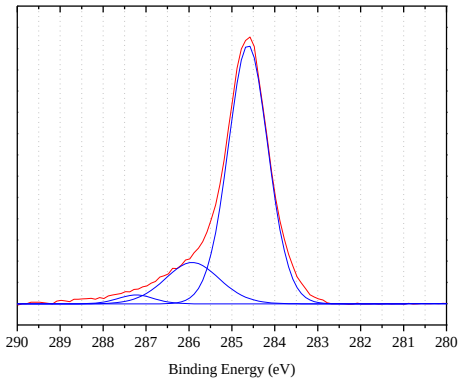

(h) ACS3 (S 2p)

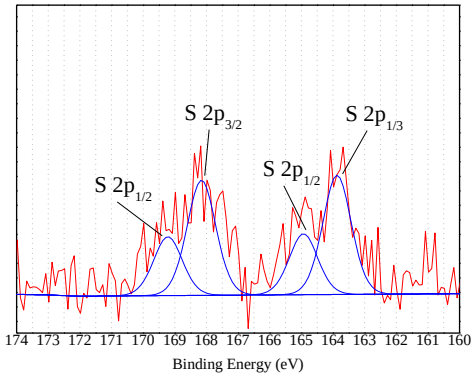

425

Figure 4

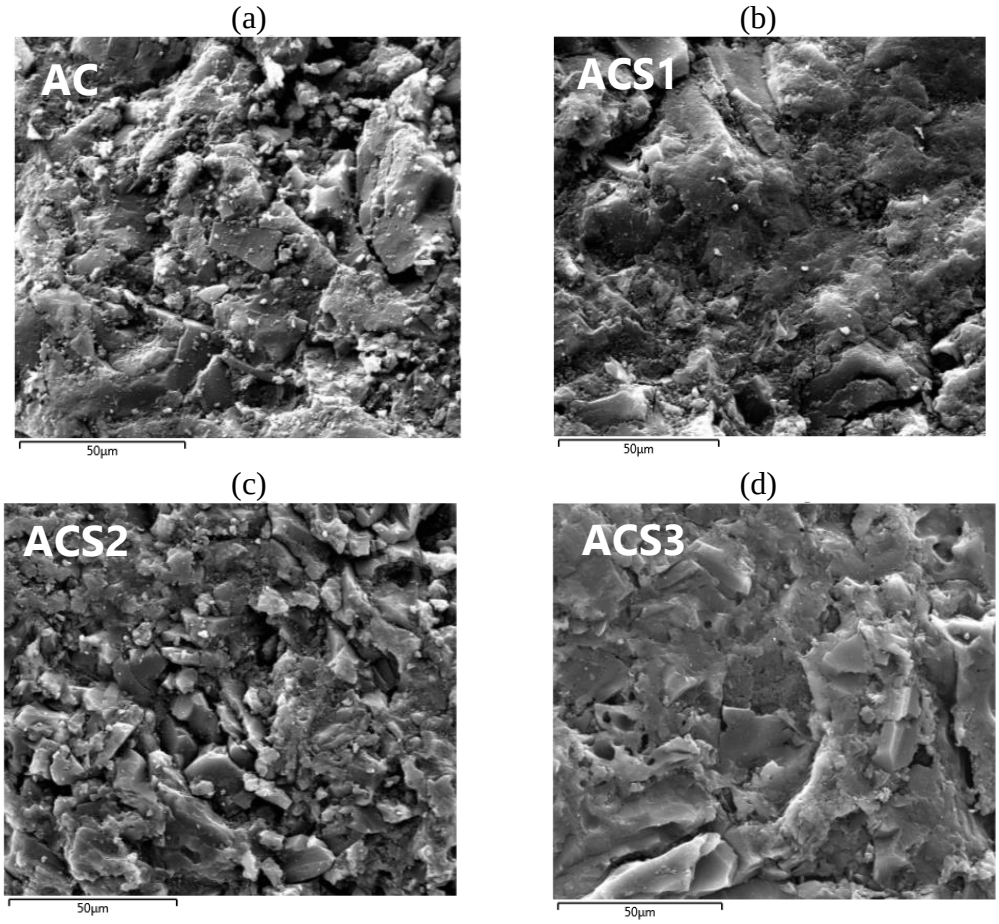

426

427 **Figure 5**

428

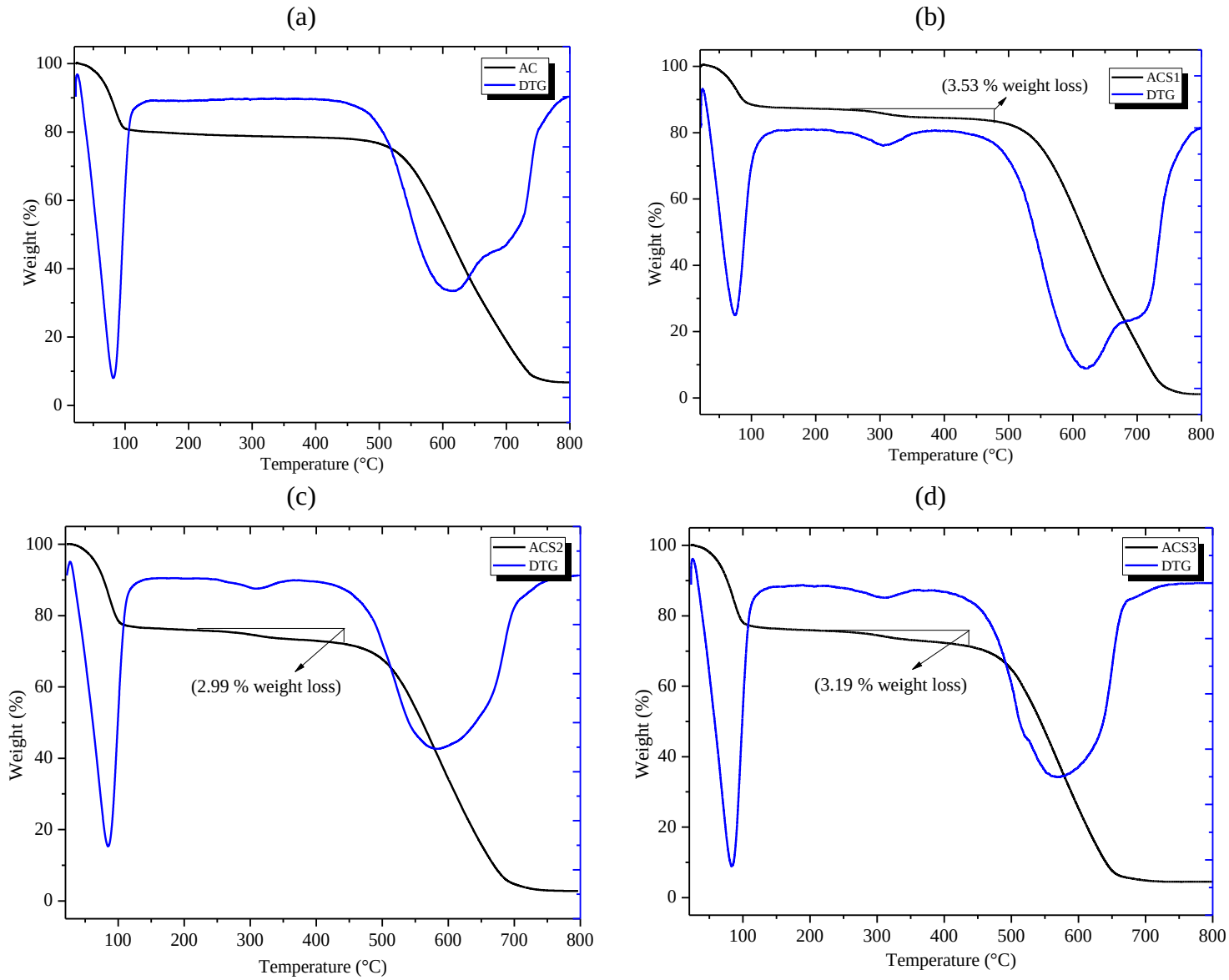

429

430 **Figure 6**

431

(a)

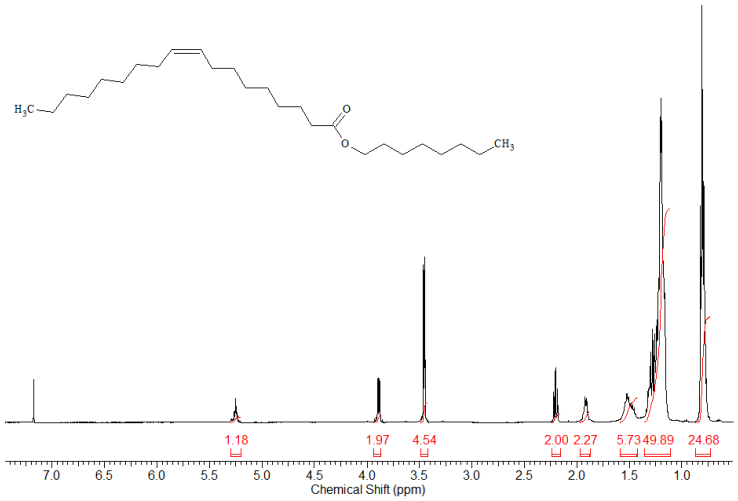
1.18
1.97
4.54
2.00
2.27
5.73
49.89
24.68
Chemical Shift (ppm)

(b)

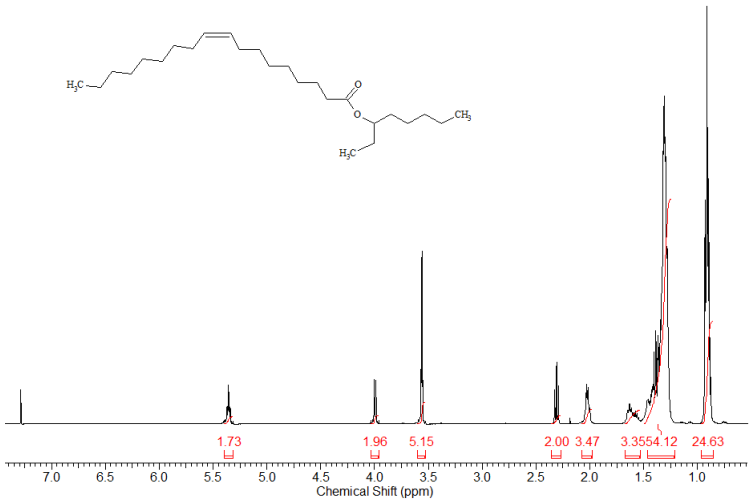
1.73
1.96
5.15
2.00
3.47
3.35
54.12
24.63
Chemical Shift (ppm)

(c)

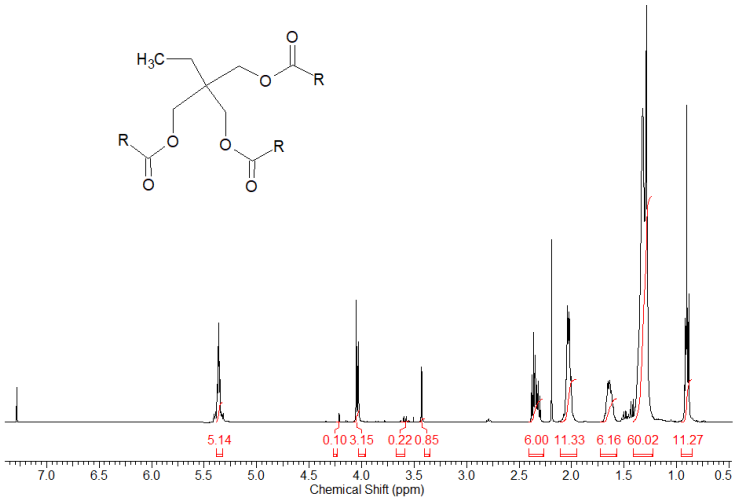
5.14
0.10
3.15
0.22
0.85
6.00
11.33
6.16
60.02
11.27
Chemical Shift (ppm)

Figure 7

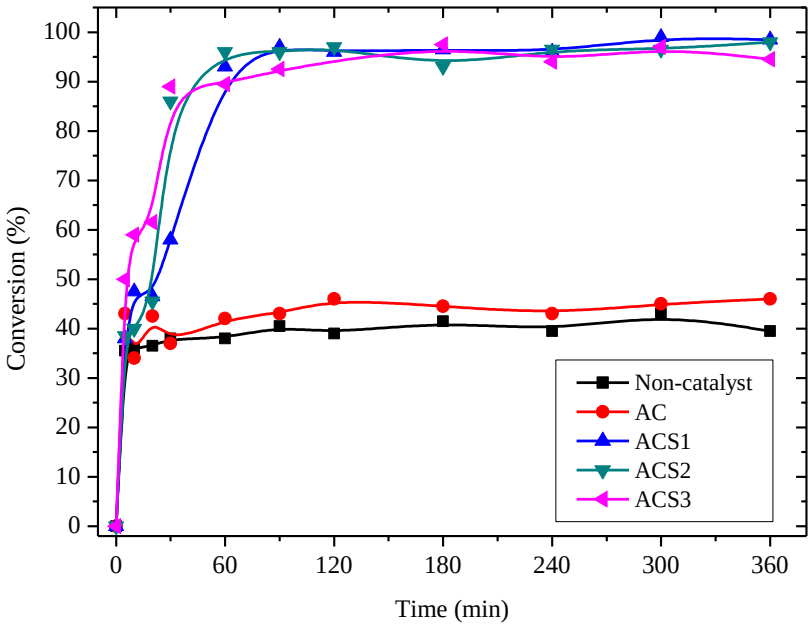

434

435 **Figure 8**

436

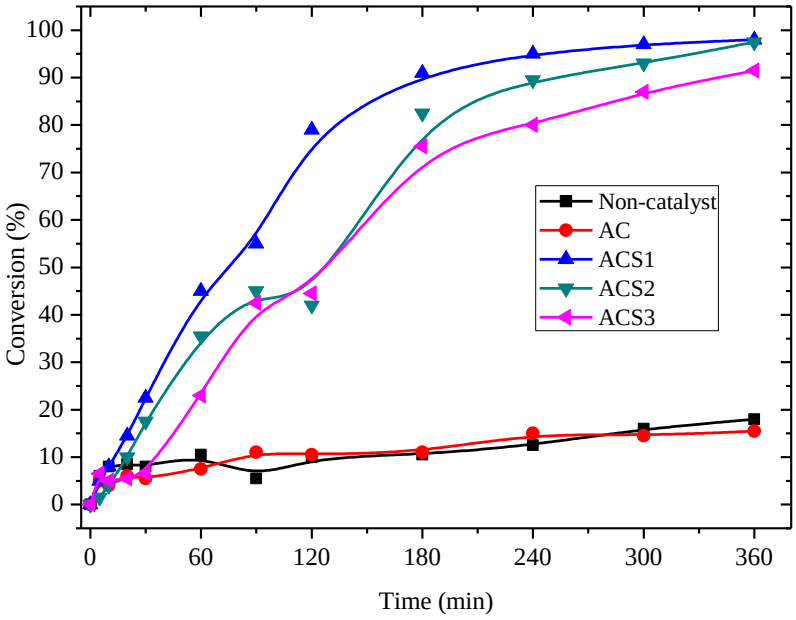

437

438 **Figure 9**

439

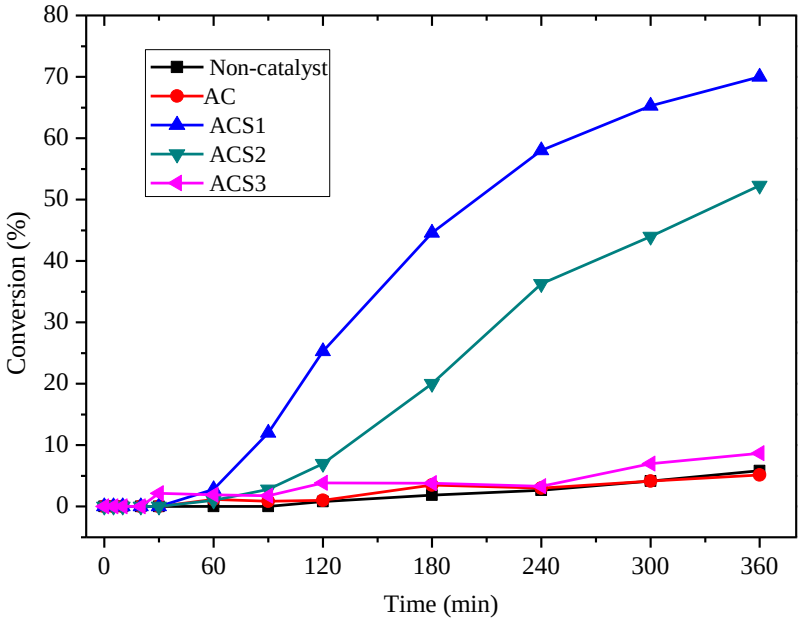

440

441 **Figure 10**

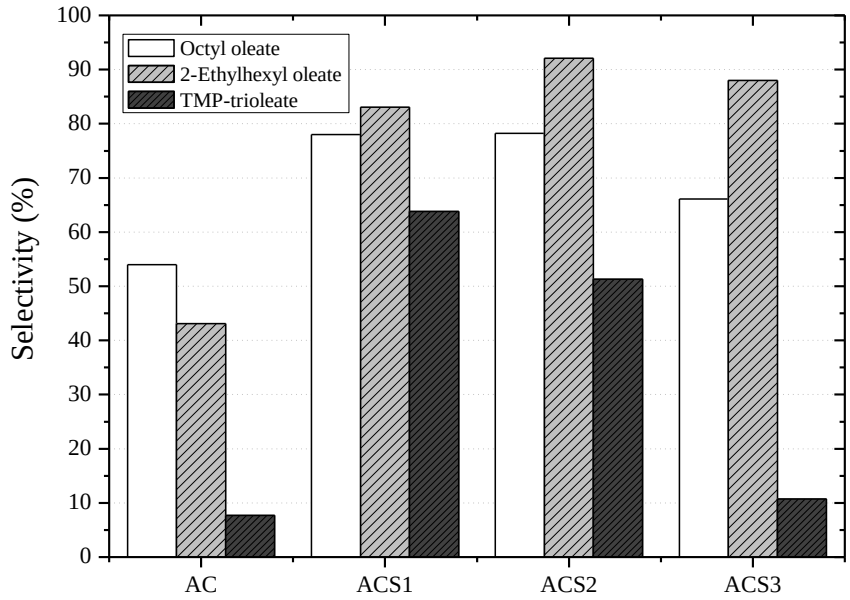

442

443 **Figure 11**